

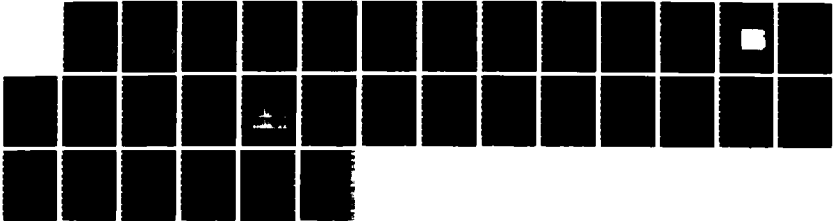
AD-A179 972

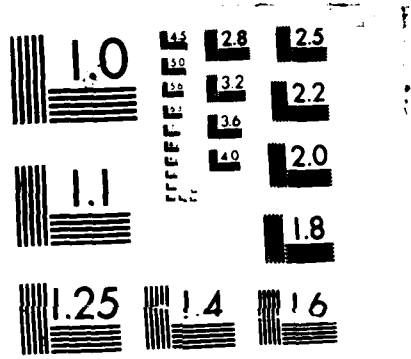
A SEARCH FOR THE PLASMA PROCESSES ASSOCIATED WITH  
PERPENDICULAR ION HEATI (U) AEROSPACE CORP EL SEGUNDO  
CA SPACE SCIENCES LAB P M KINTNER ET AL 17 FEB 87  
TR-0086(6940-06)-9 SD-TR-87-15 F/G 4/1

1/1

UNCLASSIFIED

NL





MICROCOPY RESOLUTION TEST CHART  
NATIONAL BUREAU OF STANDARDS 1963-A

DTIC FILE

12

REPORT SD-TR-87-15

AD-A179 972

# A Search for the Plasma Processes Associated with Perpendicular Ion Heating

P. M. KINTNER  
School of Electrical Engineering  
Cornell University  
Ithaca, New York 14853

and

D. J. GORNEY  
Space Sciences Laboratory  
The Aerospace Corporation  
El Segundo, California 90245-4691

17 February 1987

FINAL REPORT

Prepared for  
SPACE DIVISION  
AIR FORCE SYSTEMS COMMAND  
Los Angeles Air Force Station  
P.O. Box 92960, Worldway Postal Center  
Los Angeles, CA 90009-2960

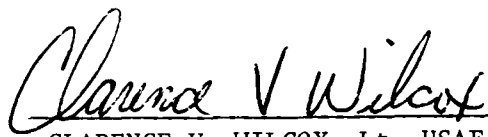
DTIC  
ELECTE  
MAY 08 1987  
S D  
E

APPROVED FOR PUBLIC RELEASE  
DISTRIBUTION UNLIMITED

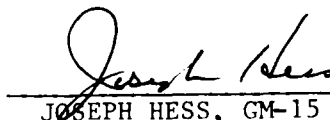
This report was submitted by The Aerospace Corporation, El Segundo, CA 90245, under Contract No. F04701-85-C-0086 with the Space Division, P. O. Box 92960, Worldway Postal Center, Los Angeles, CA 90009. It was reviewed and approved for The Aerospace Corporation by H. R. Rugge, Director, Space Sciences Laboratory. Lt Clarence V. Wilcox was the project officer for the Mission Oriented Investigation and Experimentation (MOIE) Program.

This report has been reviewed by the Public Affairs Office (PAS) and is releasable to the National Technical Information Service (NTIS). At NTIS, it will be available to the general public, including foreign nationals.

This technical report has been reviewed and is approved for publication. Publication of this report does not constitute Air Force approval of the report's findings or conclusions. It is published only for the exchange and stimulation of ideas.



CLARENCE V. WILCOX, Lt, USAF  
MOIE Project Officer  
SD/CLTP



JOSEPH HESS, GM-15  
Director, AFSTC West Coast Office  
AFSTC/WCO OL-AB

REPORT DOCUMENTATION PAGE		READ INSTRUCTIONS BEFORE COMPLETING FORM
1. REPORT NUMBER SD-TR-87-15	2. GOVT ACCESSION NO. ADA179972	3. RECIPIENT'S CATALOG NUMBER
4. TITLE (and Subtitle) A SEARCH FOR PLASMA PROCESSES ASSOCIATED WITH PERPENDICULAR ION HEATING		5. TYPE OF REPORT & PERIOD COVERED Final
		6. PERFORMING ORG. REPORT NUMBER TR-0086(6940-06)-9
7. AUTHOR(s) Paul M. Kintner (Cornell University) and David J. Gorney		8. CONTRACT OR GRANT NUMBER(s) F04701-85-C-0086
9. PERFORMING ORGANIZATION NAME AND ADDRESS The Aerospace Corporation El Segundo, CA 90245-4691		10. PROGRAM ELEMENT, PROJECT, TASK AREA & WORK UNIT NUMBERS
11. CONTROLLING OFFICE NAME AND ADDRESS Space Division Los Angeles Air Force Station Los Angeles, CA 90009-2960		12. REPORT DATE 17 February 1987
		13. NUMBER OF PAGES 28
14. MONITORING AGENCY NAME & ADDRESS (if different from Controlling Office)		15. SECURITY CLASS. (of this report) Unclassified
		15a. DECLASSIFICATION/DOWNGRADING SCHEDULE
16. DISTRIBUTION STATEMENT (of this Report)  Approved for public release; distribution unlimited.		
17. DISTRIBUTION STATEMENT (of the abstract entered in Block 20, if different from Report)		
18. SUPPLEMENTARY NOTES		
19. KEY WORDS (Continue on reverse side if necessary and identify by block number) >Aurora Ion Cyclotron Waves Ion Heating Lower-Hybrid Waves Wave-Particle Interactions, ←		
20. ABSTRACT (Continue on reverse side if necessary and identify by block number) > The satellite S3-3 data set has been examined for examples of perpendicular ion acceleration with simultaneous broadband plasma wave data. One event was found. Plasma waves in the frequency range for lower hybrid resonance (LHR) waves and in the frequency range for Doppler shifted $0^+$ ion cyclotron waves modestly correlated with the perpendicular ion acceleration, although their electric field amplitudes were less than that assumed in present theories of ion acceleration: about 0.2-6.0 mV/m (rms) for the LHR waves and 4-9 mV/m →		

## 19. KEY WORDS (Continued)

## 20. ABSTRACT (Continued)

→ (rms) for the possible Doppler shifted  $O_{\perp}^{(+)}$  cyclotron waves. Plasma waves propagating above the LHR frequency briefly reached a value of 10 mV/m (rms). No evidence was found for the existence of  $H_{\perp}^{(+)}$  cyclotron waves during the period of perpendicular ion acceleration. The thermal or superthermal electron field-aligned current density ( $E_e < 170$  eV), estimated by subtracting the current density measured by the magnetometer, correlated very well with the period of perpendicular ion acceleration.

*regards*  
*sub e*  
*20/10/19*

PREFACE

We would like to thank C. Cattell for reading the magnetometer data and M. Temerin for determining accurate S3-3 electric field experiment gains. Rob Pfaff was essential in having analog data digitized. Much of the signal processing software used in this paper was developed by R. Brittain. This research was supported at Cornell by ONR contract N0014-81-K-0018, and by U.S. Air Force Contract No. F04701-82-C-0083 at The Aerospace Corporation.

Accession For	
NTIS GRA&I	<input checked="" type="checkbox"/>
DTIC TAB	<input type="checkbox"/>
Unannounced	<input type="checkbox"/>
Justification	
By _____	
Distribution/	
Availability Codes	
Dist	Avail and/or Special
A-1	



## CONTENTS

PREFACE .....	1
I. INTRODUCTION.....	5
II. REV 752.....	7
A. Description of particle Data.....	7
B. Description of the Plasma Wave Data.....	12
C. Identification of Wave Modes.....	17
III. DISCUSSION.....	21
IV. SUMMARY AND CONCLUSIONS.....	25
REFERENCES AND BIBLIOGRAPHY.....	27



## FIGURES

1.	Proton flux, electron flux, and AC electric field.....	8
2.	Ion flux in eight energy steps, DC electric field measurement, and electron flux in eight energy steps.....	10
3.	Phase space distribution assuming $H^+$ ions.....	11
4.	Source altitude estimated from the measured ion conic pitch angle as a function of time.....	13
5.	Grey scales of plasma waves sensed by the electric V12 antenna....	14
6.	Electric field power in three frequency ranges .....	16
7.	Field-aligned current measured by the electron spectrometer and by the magnetometer.....	23

## I. INTRODUCTION

One of the major surprises in space plasma physics is that ions are commonly accelerated perpendicular to magnetic field lines to temperatures at least one hundred times larger than their initial temperatures. Experimental evidence for perpendicular ion acceleration (ion conics) has been accumulated from at least four magnetospheric satellites and two sounding rockets (Shelley et al., 1976; Sharp et al., 1977; Klumpar, 1979; Horwitz, 1980; Whalen et al., 1978, Yau et al., 1982). In contrast there exists scant evidence for the mechanism that produces perpendicular ion acceleration. The evidence that does exist suggests electrostatic (ES) ion cyclotron waves may be involved (Kintner et al., 1976; Yau et al., 1982) although this evidence is not conclusive.

In the absence of conclusive evidence for the source of perpendicular ion acceleration, a variety of theories have been developed to explain ion conic acceleration. These theoretical mechanisms fall into three categories: acceleration by ES ion cyclotron waves (Palmadesso et al., 1974; Lysak et al., 1980; Papadopoulos et al., 1980; Dusenbery and Lyons, 1981; Singh, 1981; Ashour-Abdalla et al., 1981; Okuda and Ashour-Abdalla, 1981), acceleration by ES lower hybrid (LH) waves (Chang and Coppi, 1981), and acceleration by narrow oblique potential jumps (Yang and Kan, 1983; Greenspan and Whipple, 1982). The free energy for either the ES plasma waves or potential jump must, of course, come from other sources such as field-aligned currents carried by either drifting thermal electrons or precipitating keV electrons. Those theories which employ ES waves to transfer energy imply the production of a specific type of ion conic. Namely, the accelerated ion distribution is formed nearly perpendicular to the magnetic field. After their initial acceleration the ions rise under the influence of the magnetic mirror force and form the more commonly observed ion conic with a folded (i.e., conical) distribution function. The hypothesis of nearly perpendicular acceleration is partially supported by the observation that ion conics have not been observed traveling downward. Ions accelerated by narrow, oblique potential jumps should initial-

ly have pitch angle peaked significantly away from perpendicular, and become even less perpendicular with time.

In this study we wish to identify ion acceleration regions so that simultaneous plasma wave and electric field data can be analyzed. If the perpendicular acceleration by ES waves hypothesis is correct, acceleration regions will correspond to ion distribution functions exhibiting perpendicular heating. Consequently we have exhaustively searched the particle data set from the S3-3 Aerospace ion detector for perpendicular acceleration regions with the constraint that there also exist simultaneous broad band wave data. Only one event was found, Rev 752, which we describe in this paper.

## II. REV 752

S3-3 was launched into an elliptical polar orbit with an apogee of 8000 km. The spacecraft and experiments have been described in detail elsewhere (Mozer et al., 1979). The Aerospace electrostatic ion analyzer measured positively charged particles in 8 energy steps over the range 90 eV to 3.9 keV. The angular resolution of the detector was about 10-12 degrees. Since the spacecraft was spinning in a cartwheel mode the entire range of ion pitch angles was sampled every half spin period (~ 9 seconds). The Berkeley plasma wave data described here was measured using a 36 meter double probe antenna. The analog broad band data was digitized after reception and has been reduced using standard digital signal analysis techniques.

The single event for which the ion distribution function exhibited perpendicular acceleration and for which there existed simultaneous plasma wave data occurred on Day 244 (August 31) of 1976 between 10:17:30 UT and 10:18:40 UT. S3-3 was located at 2600 km altitude, 9.1 MLT, and 77.2° invariant latitude. At this location the  $H^+$  cyclotron frequency was 320 Hz and the  $O^+$  cyclotron frequency was 20 Hz.

### A. DESCRIPTION OF PARTICLE DATA

Particle and field data from Rev 752 are summarized in Figure 1, which is a grey-scale plot of a ten-minute segment of data surrounding a day-side auroral-oval crossing. The upper panel in this figure is a frequency-time plot of the ac electric field amplitude from 32 Hz to 100 kHz. The center panel is an energy-time plot of the electron energy flux from 170 eV to 33 keV, and the lower panel is the ion energy flux for 90 eV to 3.9 keV. Narrow panels showing the observed rates in a 235 keV electron channel and a > 80 keV integral proton channel are also shown for easy orientation with respect to the high-latitude trapping boundaries. Note that these trapped particle observations show clear modulation at half the spacecraft's 18-second spin period due to low loss-cone fluxes.

# S3-3

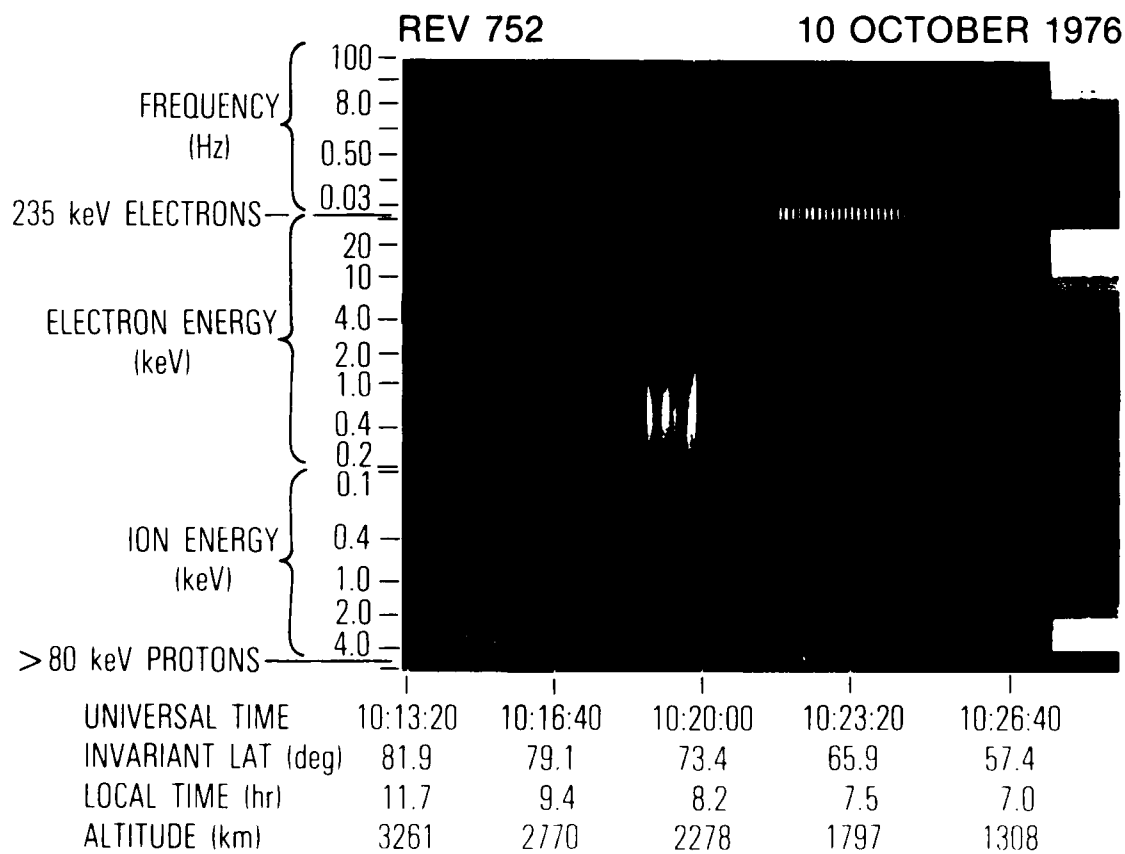


Fig. 1. Proton fluxes from 90 eV to 3.9 keV are in the bottom panel. Note the inverted energy scale. Electron fluxes from 170 eV to 33 keV are in the middle panel. The top panel is a grey scale of AC electric field from 30 Hz to 100 kHz created from broadband filter outputs.

During this ten-minute data acquisition the S3-3 spacecraft descended from  $82^\circ$  to  $66^\circ$  invariant latitude while spanning about five hours of local time (12.0 - 7.5 MLT), and dropped in altitude from 3300 kilometers to 1800 kilometers. S3-3 enters the region of interest at about 10:17:00 UT ( $\Lambda = 78.7^\circ$ ) after descending through the polar cap. The spacecraft remained on what can loosely be called auroral field lines until about 10:18:40, where it encountered a stably trapped particle population at an invariant latitude of about  $75.8^\circ$ . The ion conics were observed from about 10:17:30 to 10:18:40, during a period of intense  $\sim$  keV electron precipitation and enhanced broadband wave activity. The plasma wave observations during this period are described in the next section. The energetic particle observations from the period of interest are expanded in Figure 2.

Figure 2 shows the number flux (logarithmic) observed in each of the eight electron and proton electrostatic analyzer channels as a function of time. Also shown is the equatorward component of the dc electric field ( $E_x$ ) as observed by the Berkeley electric field probes. Vertical arrows along the abscissa indicate the times that the Aerospace electrostatic analyzers were viewing along the magnetic field direction (upward pointing arrows indicate upward viewing and vice versa). The perpendicular ion conics (called out by heavy arrows) are most easily seen as enhancements in the low energy ion flux at times when the instrument was sampling ion flux perpendicular to the magnetic field direction (between vertical arrows). The ion conic signature can be seen to extend to energies as high as 1.4 keV at times. The peak ion conic flux occurred at 10:18:13 UT, when the flux in the 90 eV channel reached  $0.5 - 1.0 \times 10^8/\text{cm}^2 \text{ sec ster keV}$ ; the flux approximately obeyed a power law with index  $P = -2$ .

The phase space distribution of the ion conic measured during the period 10:18:26 UT and 10:18:43 UT is shown in Figure 3. The ion conic flux monotonically decreased with velocity and reached maximum velocities of about 300 km/sec (about 470 eV). The flux was isotropic at higher energy levels with a loss cone in the  $-V_{\parallel}$  direction. The conic had peak fluxes very close to  $90^\circ$  pitch angle. During the period of intense ion conic fluxes (10:17:30 UT to 10:18:40 UT) the ion distribution functions had peak fluxes at  $90^\circ$  except at

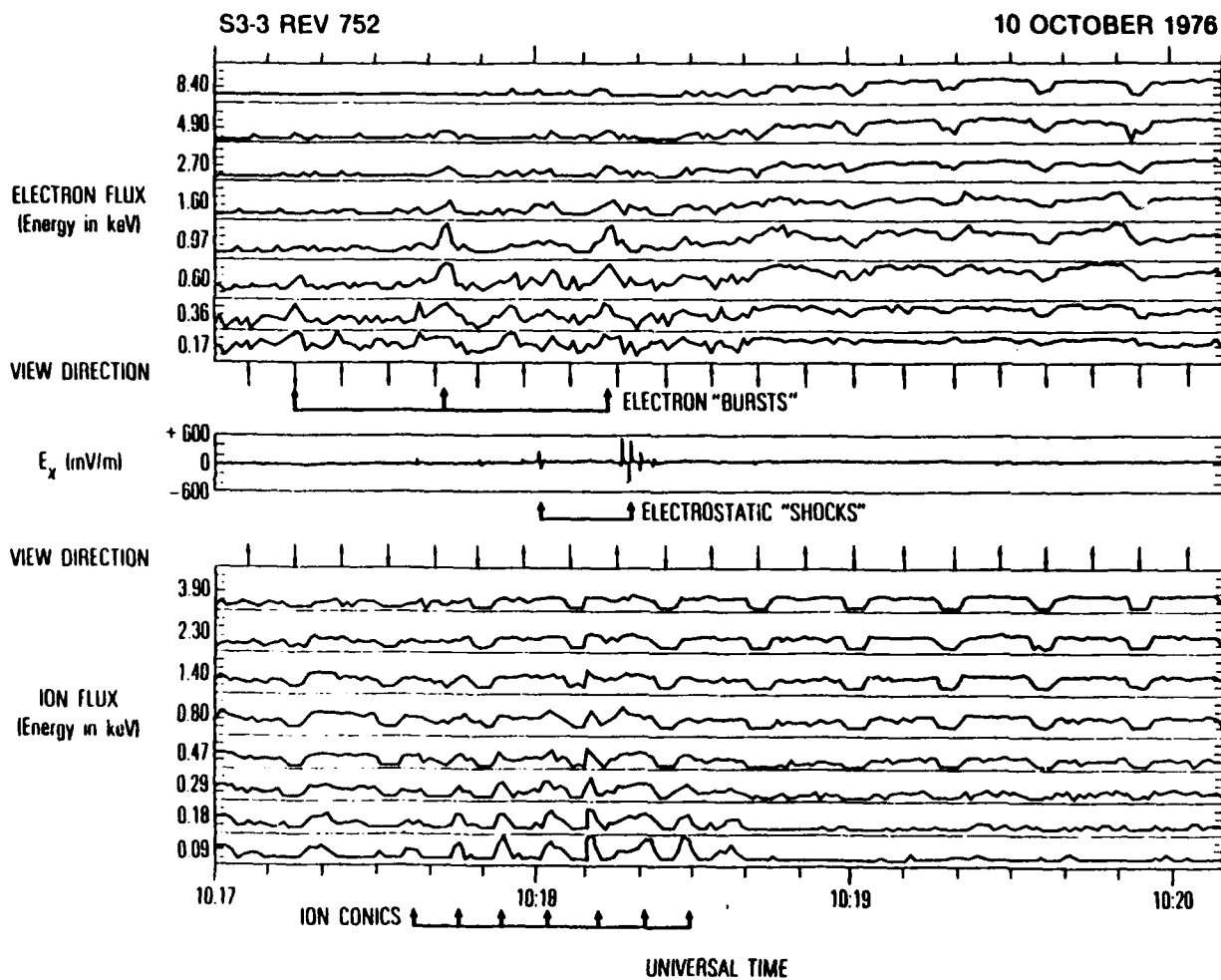


Fig. 2. The bottom panel contains the ion flux in 8 energy steps. The middle panel contains the DC electric field measurement from the V12 antenna. The top panel contains the electron flux in 8 energy steps. The view direction for both the electron and ion detectors is shown on top of the bottom panel.

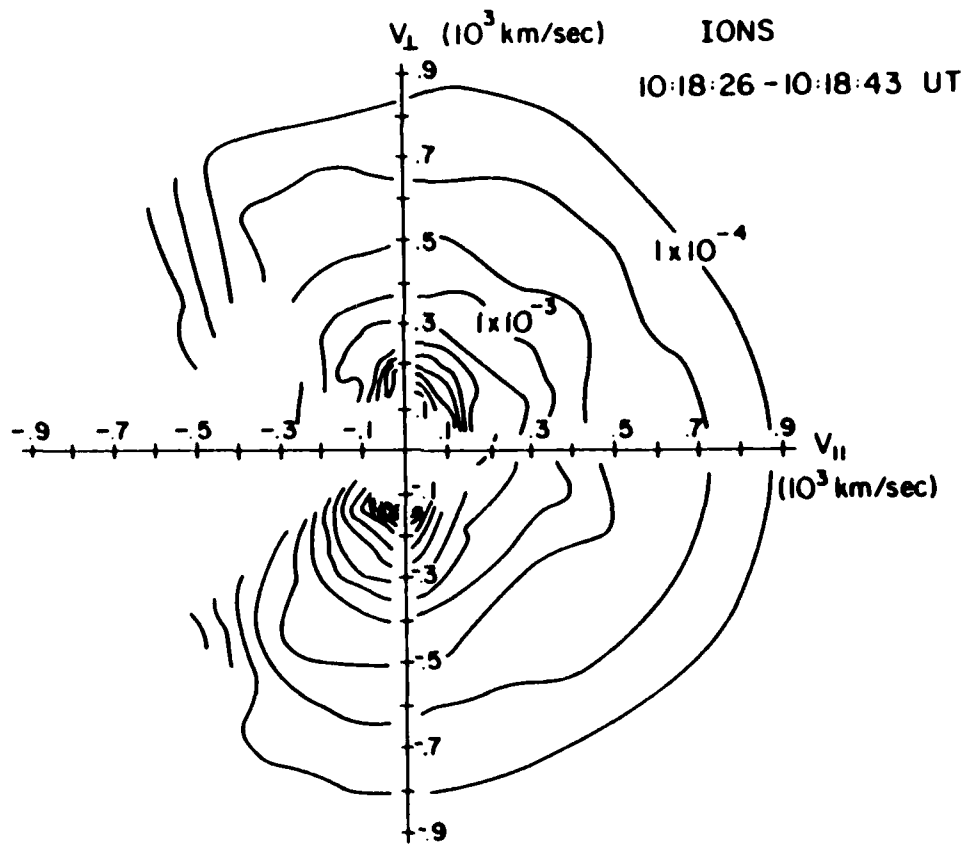


Fig. 3. The phase space distribution assuming  $H^+$  ions is shown. If the correct ion is  $O^+$  the scale values should be reduced by a factor of 4. Each line of equal density represents a step of 2.1 influx.



10:17:54 and 10:18:16 UT. Figure 4 summarizes the source altitude of each ion conic measurement assuming perpendicular generation and adiabatic motion. The source or mirror points of the ion conics thus ranged from about 2000 kilometers altitude upward to the satellite altitude thereby suggesting local ion acceleration. The atmospheric loss-cone angle through this period varied from 38° to 41°, and the ion conic signatures were located outside the loss cone. Throughout this pass, the largest conic fluxes were coincident with the lowest generation altitudes.

Sporadic enhancements of the energetic electron flux throughout the conic generation region can be seen in the upper panel of Figure 2, and in the center panel of the particle spectrogram shown in Figure 1. These electron bursts are reminiscent of the field-aligned electrons observed by Klumpar and Heikkila (1982), sometimes associated with transversely accelerated ions. Three distinct enhancements can be seen in this event, at 10:17:16, 10:17:44, and at 10:18:15 UT. The enhancement at 10:17:16 UT extends up to an energy of 600 eV, and indeed appears to be field aligned and upflowing. The bursts at 10:17:44 and 10:18:15 UT do not appear to be field aligned, and extend as high as 5 keV in energy. By comparing low energy fluxes observed by the Lockheed low energy electron detector, which lags the Aerospace detector by 90° pitch angle, with those of the Aerospace detector some information about the electron pitch angle anisotropy can be determined. In each of these three bursts, such a comparison yields results consistent with a field aligned anisotropy. It is quite likely that these (perhaps all three) electron bursts only extend over narrow, filamentary regions of space which prevents a complete sampling of their total pitch angle distribution as the spacecraft flies through at 6 km/sec. If this were the case, a latitudinal width of about 20 km or less at 2000 km altitude is implied. The highest electron flux,  $2 \times 10^8$  (cm<sup>2</sup> sec ster keV)<sup>-1</sup> at 200 eV, occurred near the center of the conic generation region.

#### B. DESCRIPTION OF THE PLASMA WAVE DATA

The plasma wave data are presented in Figure 5 where it has been divided into two panels for the purpose of examining high and low frequency waves separately. The sensor obtaining this data was the V12 double probe electric

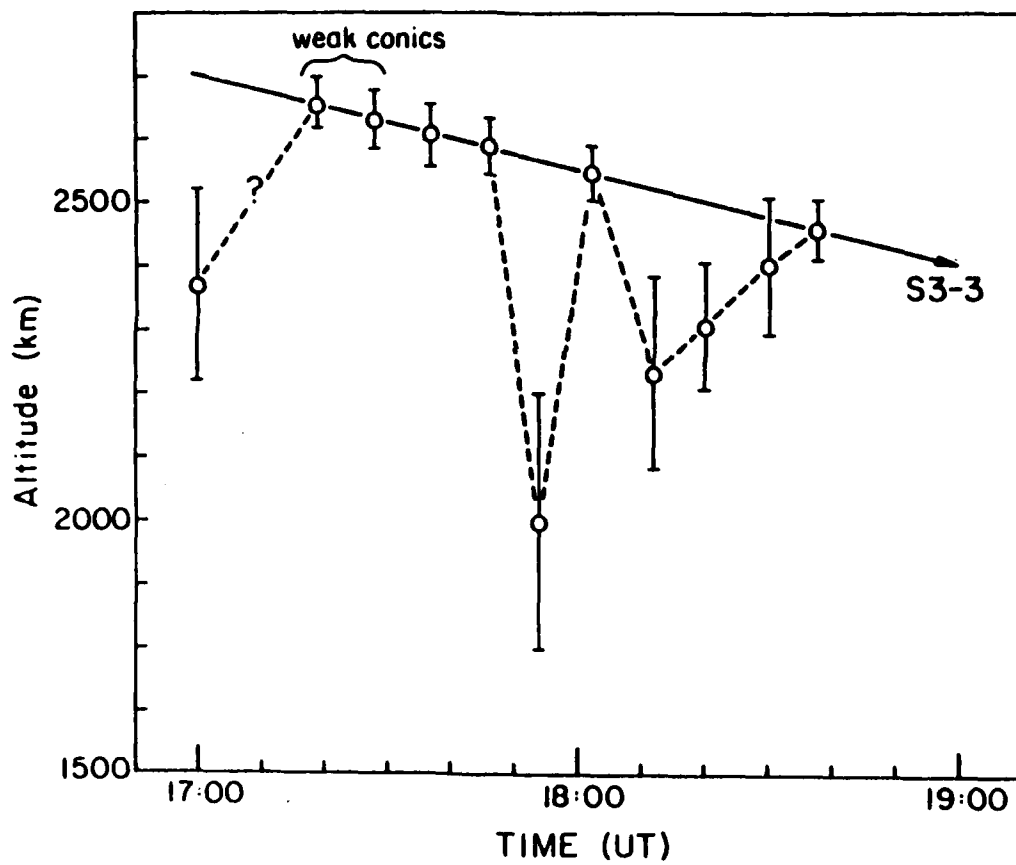


Fig. 4. Source altitude estimated from the measured ion pitch angle as a function of time. Calculation of the source altitude assumes perpendicular acceleration followed by adiabatic motion. The two points labeled weak conics were suggested by examining phase space plots but were not definitive.

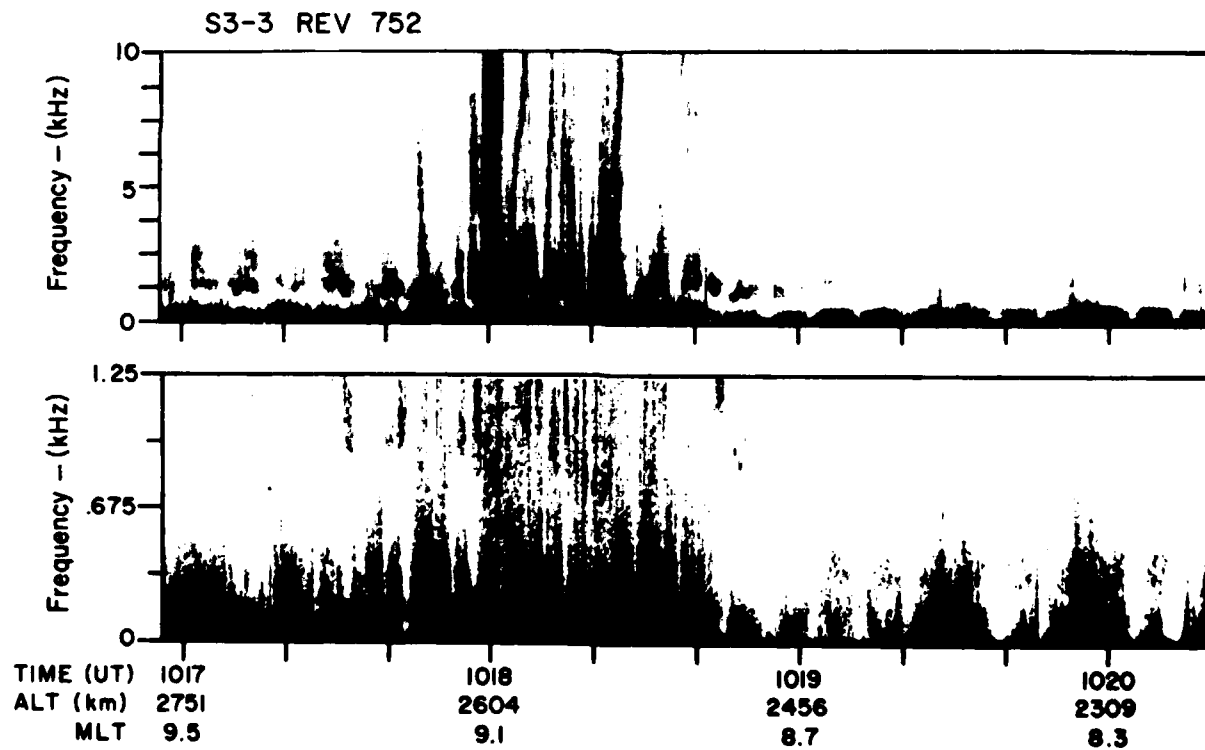


Fig. 5. Grey scales of plasma waves sensed by the electric V12 antenna. The bottom panel covers the frequency range 40 Hz - 1.25 kHz while the top panel covers the frequency range 40 Hz - 10 kHz.

antenna, which was 36 meters long and orthogonal to the S3-3 spin axis. Since the spacecraft was spinning in a cartwheel mode and since the spin axis was roughly perpendicular to the local magnetic field, the V12 antenna swept through magnetic aspect angles of  $0^\circ$  to  $360^\circ$  every spin period. We will describe the data beginning with the lowest frequencies.

Broad band unstructured turbulence below 400 Hz began before 10:17:00 UT and continued to 10:18:40 UT when it abruptly decreased. Two further bursts of turbulence occurred at 10:19:30 UT and 10:20:00 UT. The latter two bursts appear very similar to zero frequency turbulence but the earlier turbulence is more difficult to identify. Above 400 Hz there was a general increase in wave amplitude between 10:17:40 UT and 10:18:40 UT.

Narrow band emissions between 900 Hz and 1200 Hz began before 10:17:00 UT and continued to 10:19:00 UT. They were most intense between 10:17:30 UT and 10:18:45 UT. This feature can be reasonably associated with the lower hybrid frequency. At this location an LHR frequency of 1.0 kHz corresponds to a plasma density of  $400/\text{cm}^3$  assuming a predominantly oxygen plasma. This assumption is confirmed by the ion cup on S3-3 which was responding to a predominantly  $O^+$  plasma with a density of several hundred ions per  $\text{cm}^3$  during the time period 10:17:00 to 10:18:40 UT (F. Rich, personal communication, 1983). After 10:18:40 UT the ion density inferred from the ion cup dropped below  $10/\text{cm}^3$ .

Bursts of high frequency broadband waves occurred above the LHR frequency at 10:17:47 UT and at 10:18:00 UT. The latter event was quite intense and a saucer also appeared to be centered at 10:18:05 UT. The level of high frequency noise ( $f > f_{\text{LHR}}$ ) was generally more intense with some of the noise exhibiting dispersion characteristics of saucers.

To view the plasma wave data more quantitatively, it was filtered into three frequency ranges: 40-500 Hz to measure low frequency turbulence and ES ion cyclotron waves, 800-1200 Hz to measure the LHR emissions, and 2000-5000 Hz to measure the high frequency turbulence (Figure 6). For this plot we have chosen the V34 antenna, which had less gain than the V12 antenna. The lower gain antenna was less susceptible to saturation by large-amplitude fields and

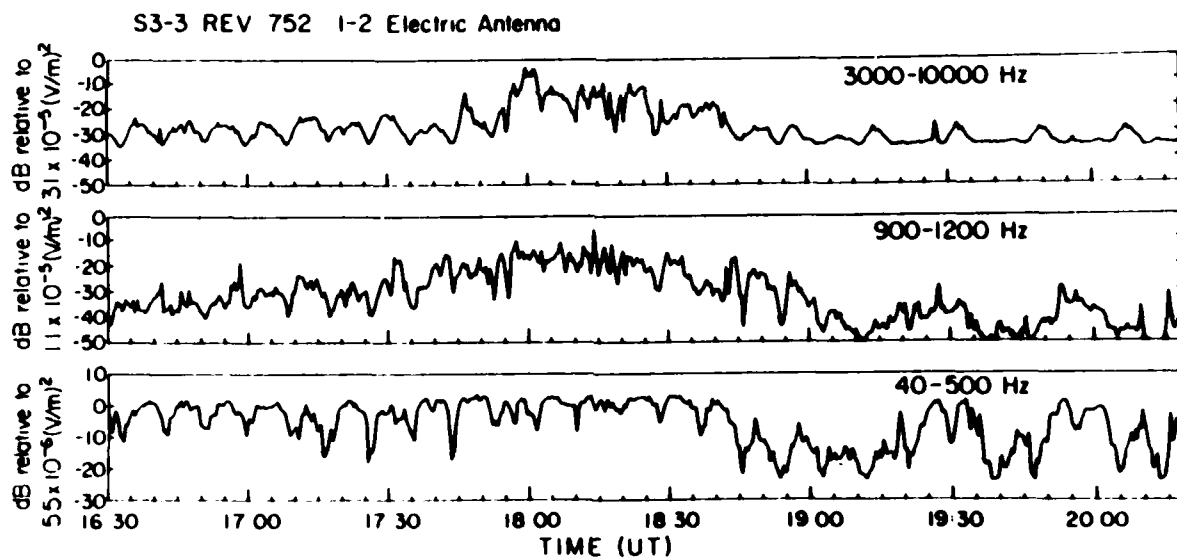


Fig. 6. Electric field power in three frequency ranges. The power is calculated by applying digital filters to the data in Figure 5. The lowest panel (40 - 500 Hz) covers the frequency range of Doppler broadened  $O^+$  and  $H^+$  ion cyclotron waves, if they exist. The middle panel (400 - 1200 Hz) covers the frequency range of LHR waves and the top panel (3 - 10 kHz) covers the frequency range of auroral hiss and saucers.

thus provided a better measure of the peak electric fields within the event. The low frequency (40-500 Hz) wave amplitude had a broad plateau beginning before 10:16:30 UT and continuing to 10:18:40 UT where the amplitude decreased dramatically. Two bursts occurred later at 10:19:30 UT and 10:20:00 UT. Periodic nulls at half the spin period (19 sec) were produced by the electric field antenna rotation with respect to the local magnetic field. There was some structure in the 40-500 Hz amplitude, which decreased around 10:17:20 UT and 10:18:40 UT. The latter period of time correlates well with the observation of conics, and we believe that the low frequency turbulence amplitude increased modestly during the period when perpendicular ion heating was observed. The broadband fields obtained were 4-6 mV/m (RMS) which occasionally peaked at 9 mV/m (RMS) over the frequency range 40 Hz - 500 Hz.

Near the LHR frequency (800 Hz - 1400 Hz) the wave amplitude began to increase around 10:17:40 UT, peaked between 10:18:00 UT and 10:18:20 UT, and then decreased rapidly around 10:18:40 UT. The more sensitive V12 antenna measured the peak between 10:18:00 UT and 10:18:20 UT to be one hundred times larger than the minimum at 10:19:00 UT and ten times larger than the values preceding the perpendicular ion acceleration. Hence the LHR noise had a broad amplitude maximum centered on the period of perpendicular ion heating. The peak fields measured were 0.2-6.0 mV/m (RMS) over the frequency range 800 - 1400 Hz.

The high frequency wave amplitude (2 kHz - 5 kHz) also increased by two orders of magnitude between 10:17:40 UT and 10:18:40 UT. The peak value at 18:00:02 UT was about 30 mV/m (RMS) over the frequency range 3 kHz to 10 kHz although a more typical value was 1 - 2 mV/m. In summary, the wave amplitude in all three frequency ranges increased in amplitude during the period of perpendicular ion heating.

#### C. IDENTIFICATION OF WAVE MODES

In the absence of severe Doppler broadening the ES ion cyclotron modes can be identified from their discrete frequency spectra. The  $H^+$  and  $O^+$  cyclotron frequencies were 320 Hz and 20 Hz, respectively. The ES ion cyclotron phase velocity should be the order of three to five times the ion thermal

velocity ( $V_{ph}^2 = (\frac{\omega ci}{k})^2 + C_s^2$ ). For 3000 °K plasma the  $H^+$  thermal velocity is 1.26 km/sec while the  $O^+$  thermal velocity is .32 km/sec. The spacecraft velocity was about 7 km/sec. The electrostatic hydrogen cyclotron wave would have been broadened but not beyond recognition. If the ESHC waves existed in any sense similar to previous observations (Kintner et al., 1978), they should have been observable in this data. We conclude that no ES hydrogen cyclotron waves existed during the period of perpendicular ion heating. It is conceivable that oxygen cyclotron waves were Doppler broadened beyond recognition. The wave data were carefully examined for structures with a characteristic frequency of 20 Hz and none were found. If they were Doppler broadened they may have accounted for the low frequency turbulence up to 400 Hz. Unfortunately, Doppler shifted zero-frequency turbulence (Temerin, 1978) could also have accounted for the observed low frequency power. Zero-frequency turbulence is known to be the most common auroral zone feature in this frequency range. If all observed power below 500 Hz is interpreted as being produced by  $O^+$  cyclotron waves, an upper limit on the average  $O^+$  wave amplitude during perpendicular ion heating was 4-9 mV/m (RMS).

Waves near the lower hybrid frequency can exist in at least two different modes. The first mode is the long wavelength electromagnetic wave. As the electromagnetic mode approaches resonance, the ratio E/B increases rapidly and, although the Poynting vector remains unchanged, the electric field amplitude increases which gives a quasi-electrostatic character to the wave. The second mode is mostly electrostatic. This is one of the modes predicted to be produced by precipitating electrons and to heat ions perpendicular to the magnetic field (Chang and Coppi, 1981). It is not possible to distinguish the two wave modes in our data. Since the purely electrostatic mode does not propagate away from its source, the observation of simultaneous precipitating electrons would support that mode's existence. The three electron bursts (17:16, 17:44, and 18:15 UT) are a possible source of free energy but the largest amplitude LHR waves only roughly correlate with these times.

At frequencies higher than the LHR frequency, Basu et al. (1982) predict the existence of electrostatic modes with wavelengths the order of the ion gyroradius -- LH waves as opposed to LHR waves. They further suggest that LH

waves can significantly accelerate ions in the perpendicular direction. The high frequency noise observed between 10:17:40 UT and 10:18:40 UT may have been electrostatic LH mode, or it may have been electromagnetic saucers (James, 1976).

In conclusion, it is possible that oxygen cyclotron waves or electrostatic LHR waves existed during the period of perpendicular ion heating. The spectral evidence for the LHR waves is stronger but the existence of  $O^+$  cyclotron waves cannot be dismissed. No evidence existed for the presence of the ES hydrogen cyclotron waves. At higher frequencies the data suggests the existence of either an electrostatic LH mode or an electromagnetic saucer.



### III. DISCUSSION

We have presented a clear example of perpendicular ion conics with no clear example of the driving mechanism. If plasma waves were the acceleration mechanism, we might expect them to increase in amplitude at 10:17:30 UT and to decrease at 10:18:40 UT. The low frequency waves ( $< 500$  Hz) satisfied the latter condition at 10:18:40 UT but they exhibited only a modest increase after 10:17:30 UT. The LHR waves and LH waves increased gradually after 10:17:30 UT and peaked near 10:18:00 UT. They decreased gradually after 10:18:30 UT until 10:19:00 UT. Hence, the spatial/temporal correlation of the low frequency waves, the LHR waves or the LH waves with the ion conics was suggestive but not conclusive. In all cases the correlation may have been distorted by the existence of plasma waves in the same frequency range, which do not accelerate ions (zero frequency turbulence, EM-LHR waves or EM-saucers).

If, for the moment, we accept the existence of one of the two modes (ES  $O^+$  cyclotron wave or ES-LH wave) during the period of perpendicular ion acceleration, we may examine the measured wave amplitude for consistency with the several theories of ion conic generation. For example, Dusenbery and Lyons (1981) predict that ion cyclotron wave amplitudes of 10 - 20 mV/m will accelerate ions (quasilinearly) up to 40 times their initial energy. The observed wave amplitude (4 - 9 mV/m) is too small and the observed ion energy (400 eV) implies an acceleration on the order of 400 times or more of the initial ion energy. Lysak et al. (1980), by not making the random phase approximation, predict ion conic energies of 400 eV but this theory requires ion cyclotron waves with electric field amplitudes of 100 mV/m. In this case the observed low frequency wave amplitude, if interpreted as being produced by  $O^+$  cyclotron waves, is also too small. For LHR wave acceleration mechanisms, Chang and Coppi (1981) assume an amplitude of 50 mV/m compared to the observed value of 0.2 - 6.0 mV/m. If their theory is extended to include the frequencies above the LHR resonance, the peak observed amplitude is unchanged except near 18:18:02, where it briefly reaches 30 mV/m (rms). In general, the observed electric field amplitudes appear to be too small to satisfy these theories.

We can think of two explanations for the weak signal amplitude between 40 Hz and 500 Hz. First, it is possible that the  $O^+$  cyclotron wave phase velocity is much larger than the spacecraft velocity and no Doppler shifting occurred. However, this implies that the  $O^+$  temperature should be the order of 100 eV, which does not seem likely. Second, it is possible that the  $O^+$  cyclotron wavelength was small compared to the electric antenna length (37 m). However, the  $O^+$  gyroradius was 12 meters, assuming an ion temperature of 3000°K, which implies a wavelength of about 80 meters ( $kp_1 = 1$ ). Further, we examined the V56 antenna, whose length was 6 meters, and calculated signal amplitudes between 40 Hz and 500 Hz that were consistent with the longer antennas. The shorter V56 antenna also measured amplitudes at the LHR frequency that were consistent with the longer antennas.

Thus far we have not discussed the source of free energy for perpendicular ion heating. Since virtually every theory uses some form of field-aligned electron motion, we have examined the electron spectrometer and the magnetometer for evidence of field-aligned current. The electron spectrometer measured the energetic electron distribution ( $> 170$  eV) while the S3-3 magnetometer measured the overall field-aligned current produced both by drifting thermal electrons and energetic electrons. The current inferred from both measurements is shown in Figure 7.

We define field-aligned as positive in the same direction as the local magnetic field (downward). The precipitating electrons carried an upward (negative) current over the region of interest while the integrated current distribution measured by the magnetometer was downward (positive). Both measurements roughly correlate in time with the observations of ion conics. Large positive currents measured by the magnetometer began at 10:17:00 UT and ended about 10:18:30 UT while the energetic electron current was negative and sometimes large from 10:17:30 to 10:18:30 UT. Both techniques indicate a large change in measured current when the ion conic observations ceased at about 10:18:40 UT. Since the magnetometer integrates electron current over all electron energies while the electron spectrometer only senses electrons with energies greater than or equal to 170 eV, an estimate of the current carried by cold electrons ( $E_e < 170$  eV) can be obtained by subtracting the

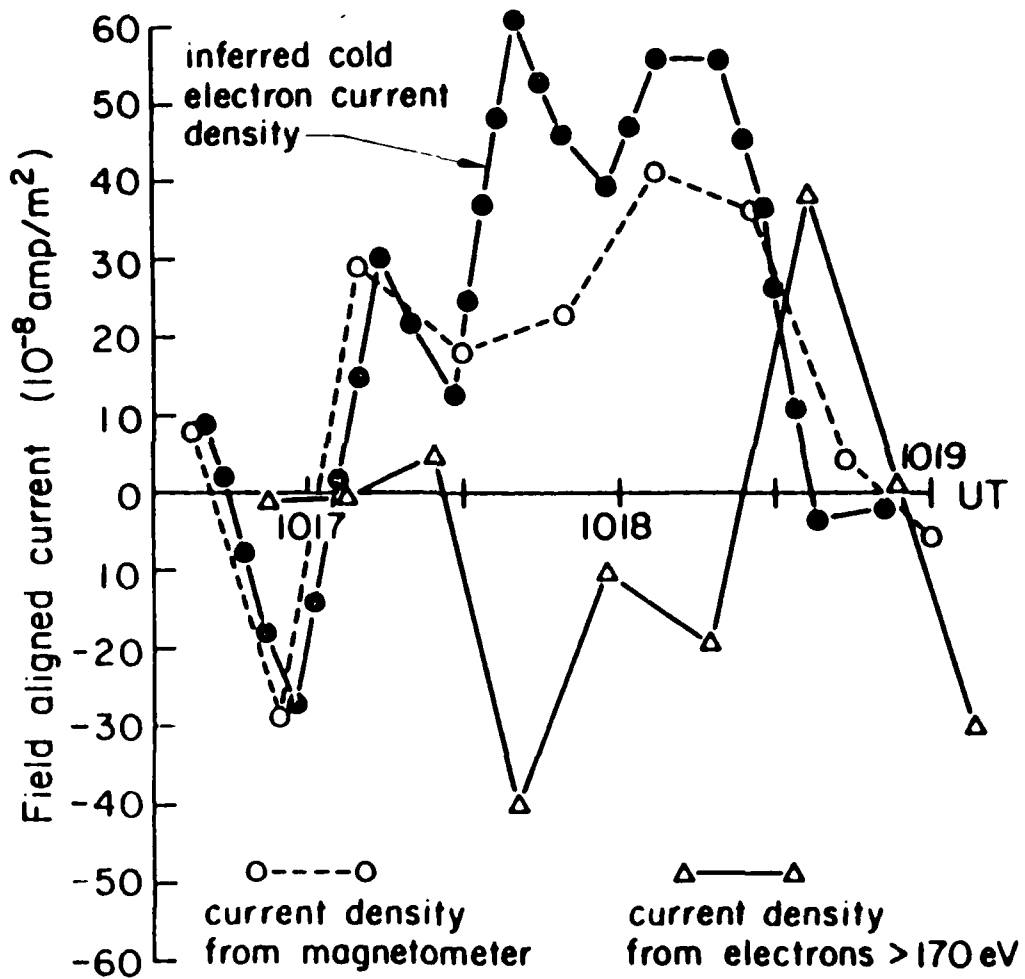


Fig. 7. Field-aligned current measured by the electron spectrometer and by the magnetometer. The cold electron current density ( $E_e < 170$  eV) is estimated by subtracting the electron spectrometer measurement from the magnetometer measurement.

current measured by the electron spectrometer from that measured by the magnetometer. The result is labeled in Figure 7 as "inferred cold electron current density." It is very large and correlates very well with the presence of ion conics. Of all the physical parameters examined the inferred cold electron current density correlated best with the presence of perpendicular ion heating.

If the inferred cold electron current density was produced by drift in the entire thermal electron population, we can estimate the drift speed. The electron density is known from the LHR frequency to be about  $400/\text{cm}^3$ . This implies that the thermal electron drift velocity was  $7.8 \times 10^3$  m/sec for  $J = .5 \mu\text{amp}/\text{m}^2$ . The electron thermal velocity for a temperature of  $3000^\circ\text{K}$  is about  $3.2 \times 10^5$  m/sec, and consequently, the ratio of the drift velocity to the thermal velocity is small, about  $2.4 \times 10^{-2}$ . If the electron and ion temperatures are equal, this field aligned current is stable (Kindel and Kennel, 1971). For instability in an  $\text{O}^+$  plasma, the velocity ratio should exceed  $1 \times 10^{-1}$ ; an  $\text{H}^+$  plasma is even more stable. The modest increase in plasma wave activity during this period was probably not produced by a drifting thermal electron population, and we suspect that other nonthermal features of the plasma distribution function were responsible for the plasma waves.

#### IV. SUMMARY AND CONCLUSIONS

Using the hypothesis the ion conics are produced by perpendicular ion acceleration, we searched the S3-3 data for examples of ion distribution functions peaked in the perpendicular direction which coincided with the existence of broadband plasma wave data. One example was found.

During the period of perpendicular ion acceleration the plasma wave data were examined closely. Plasma waves were identified at the LHR frequency and above the LHR frequency although we were unable to distinguish electromagnetic modes from electrostatic modes. The LHR wave amplitude was 0.2 - 6.0 mV/m over the frequency range 800 - 1400 Hz. At frequencies greater than the LHR frequency the peak wave amplitude was 30 mV/m. If  $O^+$  ion cyclotron waves existed, they would have been Doppler broadened into the frequency range below 500 Hz. In that case their amplitude was about 4 - 9 mV/m. Because zero-frequency turbulence is also Doppler broadened in the frequency range below 500 Hz we could not identify the wave mode. Both the LHR or LH waves and the waves below 500 Hz correlated modestly with the presence of perpendicular ion acceleration. The electric field amplitudes for all cases were too small for present theories for perpendicular ion acceleration. No evidence was found for the existence of  $H^+$  cyclotron waves during the entire event.

The source of free energy for the ion acceleration was examined by using the energetic electron spectrometer and the magnetometer. The physical parameter that correlated best with perpendicular ion acceleration was the field-aligned current carried by electrons with energies less than 170 eV. A current of  $.5 \mu\text{amp}/\text{m}^2$  was estimated which implied thermal electron drift velocities equal to  $2.4 \times 10^{-2}$  of the electron thermal velocity. This drift velocity is stable to electrostatic ion cyclotron waves.

It is perhaps somewhat risky to generalize from the results of one event. Yet this is the only event in the entire S3-3 set where perpendicular ion heating and broadband wave data are available. Other active spacecraft either have an unsatisfactory orbit or lack the necessary instrumentation to study this topic. Further progress must await new experiments which are

capable of measuring plasma wave phase velocities directly and will remove the ambiguity in determining wave modes. Regardless of which wave modes are present, the electric field amplitudes appear small.

## REFERENCES AND BIBLIOGRAPHY

- Ashour-Abdalla, M., H. Okuda and C. Z. Cheng, Acceleration of heavy ions on auroral field lines, Geophys. Res. Lett., 8, 795, 1981.
- Basu, B., T. Chang and B. Coppi, Energization of ions by long wavelength lower hybrid waves, Proceeding of the International Conference on Plasma Physics, Göteborg, Sweden, 1982.
- Chang, T. and B. Coppi, Lower hybrid acceleration and ion evolution in the supra-auroral region, Geophys. Res. Lett., 8, 1253, 1981.
- Dakin, D. R., T. Tajima, G. Benford and N. Rynn, Ion heating by the electrostatic ion cyclotron instability: theory and experiment, J. Plasma Phys., 15, 175, 1976.
- Dusenbery, P. B. and L. R. Lyons, Generation of ion-conic distribution by upgoing ionospheric electrons, J. Geophys. Res., 86, 7627, 1981.
- Greenspan, M. E. and E. C. Whipple, The effect of oblique double layers on particle magnetic moment and gyrophase, Yosemite Conference on Origins of Plasmas and Electric Fields in the Magnetosphere, Yosemite, California, 1982.
- Horwitz, J. L., Conical distributions of low-energy ion fluxes at synchronous orbit, J. Geophys. Res., 85, 2057, 1980.
- James, H. G., VLF saucers, J. Geophys. Res., 81, 501, 1976.
- Kindel, J. M. and C. F. Kennel, Topside current instabilities, J. Geophys. Res., 76, 3055, 1971.
- Kintner, P. M., M. C. Kelley and F. S. Mozer, Electrostatic hydrogen cyclotron waves near one earth radius altitude in the polar magnetosphere, Geophys. Res. Lett., 5, 129, 1978.
- Klumpar, D. M., Transversely accelerated ions: an ionospheric source of hot magnetospheric ions, J. Geophys. Res., 84, 7201, 1979.
- Klumpar, D. M. and W. J. Heikkila, Electrons in the ionospheric loss cone: evidence for runaway electrons as carriers of downward Birkeland currents, Geophys. Res. Lett., 9, 873, 1982.
- Lysak, R. L., M. K. Hudson and M. Temerin, Ion heating by strong electrostatic ion cyclotron turbulence, J. Geophys. Res., 85, 678, 1980.

- Mozer, F. S., C. A. Cattell, M. Temerin, R. B. Torbert, S. Von Glinski, M. Waldorff and J. Wygant, The dc and ac electric field, plasma density, plasma temperature, and field-aligned current experiments on the S3-3 satellite, J. Geophys. Res., 84, 5875, 1979.
- Okuda, H. and M. Ashour-Abdalla, Formation of a conical distribution and intense ion heating in the presence of hydrogen cyclotron waves, Geophys. Res. Lett., 8, 811, 1981.
- Palmadesso, P. J., T. P. Coffey, S. L. Ossakow and K. Papadopoulos, Topside ionospheric ion heating due to electrostatic ion cyclotron turbulence, Geophys. Res. Lett., 3, 105, 1974.
- Papadopoulos, K., J. D. Gaffey, Jr. and D. J. Palmadesso, Stochastic acceleration of large M/Q ions by hydrogen cyclotron waves in the magnetosphere, Geophys. Res. Lett., 7, 1014, 1980.
- Sharp, R. D., R. G. Johnson and E. G. Shelley, Observation of an ionospheric acceleration mechanism producing energetic (keV) ions primarily normal to the geomagnetic field direction, J. Geophys. Res., 82, 3324, 1977.
- Shelley, E. G., R. D. Sharp and R. G. Johnson, Satellite observations of an ionospheric acceleration mechanism, Geophys. Res. Lett., 3, 654, 1976.
- Singh, N., R. W. Schenk and J. J. Sojka, Energization of ionospheric ions by electrostatic hydrogen cyclotron waves, Geophys. Res. Lett., 8, 1249, 1981.
- Temerin, M. A., The polarization, frequency and wavelength of high-altitude turbulence, J. Geophys. Res., 83, 2609, 1978.
- Temerin, M. A., C. Cattell, R. Lysak, M. Hudson, R. B. Torbert, F. S. Mozer, R. D. Sharp and P. M. Kintner, The small-scale structure of electrostatic shocks, J. Geophys. Res., 86, 278, 1981.
- Whalen, B. A., W. Bernstein and D. W. Daly, Low altitude acceleration of ionospheric ions, Geophys. Res. Lett., 5, 55, 1978.
- Yang, W. H. and J. R. Kan, Generation of conic ions by auroral electric fields, J. Geophys. Res., 88, 465, 1983.



## LABORATORY OPERATIONS

The Aerospace Corporation functions as an "architect-engineer" for national security projects, specializing in advanced military space systems. Providing research support, the corporation's Laboratory Operations conducts experimental and theoretical investigations that focus on the application of scientific and technical advances to such systems. Vital to the success of these investigations is the technical staff's wide-ranging expertise and its ability to stay current with new developments. This expertise is enhanced by a research program aimed at dealing with the many problems associated with rapidly evolving space systems. Contributing their capabilities to the research effort are these individual laboratories:

Aerophysics Laboratory: Launch vehicle and reentry fluid mechanics, heat transfer and flight dynamics; chemical and electric propulsion, propellant chemistry, chemical dynamics, environmental chemistry, trace detection; spacecraft structural mechanics, contamination, thermal and structural control; high temperature thermomechanics, gas kinetics and radiation; cw and pulsed chemical and excimer laser development including chemical kinetics, spectroscopy, optical resonators, beam control, atmospheric propagation, laser effects and countermeasures.

Chemistry and Physics Laboratory: Atmospheric chemical reactions, atmospheric optics, light scattering, state-specific chemical reactions and radiative signatures of missile plumes, sensor out-of-field-of-view rejection, applied laser spectroscopy, laser chemistry, laser optoelectronics, solar cell physics, battery electrochemistry, space vacuum and radiation effects on materials, lubrication and surface phenomena, thermionic emission, photo-sensitive materials and detectors, atomic frequency standards, and environmental chemistry.

Computer Science Laboratory: Program verification, program translation, performance-sensitive system design, distributed architectures for spaceborne computers, fault-tolerant computer systems, artificial intelligence, micro-electronics applications, communication protocols, and computer security.

Electronics Research Laboratory: Microelectronics, solid-state device physics, compound semiconductors, radiation hardening; electro-optics, quantum electronics, solid-state lasers, optical propagation and communications; microwave semiconductor devices, microwave/millimeter wave measurements, diagnostics and radiometry, microwave/millimeter wave thermionic devices; atomic time and frequency standards; antennas, rf systems, electromagnetic propagation phenomena, space communication systems.

Materials Sciences Laboratory: Development of new materials: metals, alloys, ceramics, polymers and their composites, and new forms of carbon; non-destructive evaluation, component failure analysis and reliability; fracture mechanics and stress corrosion; analysis and evaluation of materials at cryogenic and elevated temperatures as well as in space and enemy-induced environments.

Space Sciences Laboratory: Magnetospheric, auroral and cosmic ray physics, wave-particle interactions, magnetospheric plasma waves; atmospheric and ionospheric physics, density and composition of the upper atmosphere, remote sensing using atmospheric radiation; solar physics, infrared astronomy, infrared signature analysis; effects of solar activity, magnetic storms and nuclear explosions on the earth's atmosphere, ionosphere and magnetosphere; effects of electromagnetic and particulate radiations on space systems; space instrumentation.

...

END

6-87

DTIC